A microemulsion preparation of nanoparticles of europium in silica with luminescence enhancement using silver

2009 Nanotechnology 20 085608

(http://iopscience.iop.org/0957-4484/20/8/085608)

Nanotechnology **20** (2009) 085608 (7pp) doi:10.1088/0957-4484/20/8/085608

A microemulsion preparation of nanoparticles of europium in silica with luminescence enhancement using silver

Zhi Ya Ma, Dosi Dosev and Ian M Kennedy[1]

Department of Mechanical and Aeronautical Engineering, University of California Davis, CA 95616, USA

E-mail: imkennedy@ucdavis.edu

Received 11 October 2008, in final form 10 January 2009
Published 3 February 2009
Online at stacks.iop.org/Nano/20/085608

Abstract

A facile one-pot microemulsion method has been developed for the synthesis of spherical silver core–silica shell ($Ag@SiO_2$) nanoparticles with europium chelates doped in the shell through a silane agent. The method is significantly more straightforward than other extant methods. Measurements of the luminescent emissions from the $Ag@SiO_2$ nanoparticles, in comparison with control silica nanoparticles without silver cores, showed that the presence of the silver cores can increase the fluorescence intensity approximately 24-fold and decrease the luminescence lifetime. This enhancement offers a potential increase in overall particle detectability with increased fluorophore photostability.

1. Introduction

Metal enhanced fluorescence (MEF) has attracted considerable interest in the past five years because of the widespread use of molecular fluorescence-based measurements and devices in chemistry, molecular biology, materials science, photonics, and medicine [1–5]. MEF has been used as a powerful technology to increase the sensitivity of target molecule detection in biological assays, such as DNA/RNA detection [6, 7] and immunoassays [8, 9]. The effect of MEF has been intensively studied [10–12]. MEF is believed to occur due to a coupling of the fluorophore with the plasmon resonance of a metal nanoparticle (silver or gold); the enhancement depends on many factors, such as the metal particle size and shape, the orientation of the fluorophore, dipole moments relative to the metal nanoparticles, metal–fluorophore distance, and the radiative decay rate and quantum yield of the fluorophore. The interactions of fluorophores with metal nanoparticles result in fluorescence enhancement, increased photostability, decreased lifetimes due to increased rates of system radiative decay and increased transfer distances for fluorescence resonance energy transfer [13, 14].

Most studies that have demonstrated MEF were carried out on two-dimensional surfaces, where glass microscope slides [15, 16] or plastics [17] were used as the primary substrates, and silver nanostructures, including silver island films [18], silver colloids [19], silver nanorods [20] or silver fractals [21] were deposited using wet chemistry [22], electroplating, light-assisted deposition [23] or lithographical methods [24]. Only a few studies have reported the use of colloid-based systems. For example, biotinylated silver core–silica shell ($Ag@SiO_2$) nanoparticles aggregated with Cy3-labeled streptavidin in suspension as a solution-based fluorescence sensing platform showed a 3–5-fold enhancement [25]. Later, various fluorophore-doped $Ag@SiO_2$ core–shell nanocomposites were developed by the same group and these nanocomposites could be used as a useful platform for MEF and single nanoparticle sensing [26]. The observation of enhancement of fluorescence by nanocomposites consisting of a gold core, a silica-spacer shell of variable thickness, and a dye-labeled shell was also reported recently [27]. However, both of these silver–silica core–shell nanoparticles were prepared with a laborious procedure which involved at least three steps: preparation of silver colloids by chemical reduction of silver ions; growth of silica shells of various thicknesses on the silver surface; and doping or covalent linking of fluorophores to the silica shell. In order to grow the silica shell on the silver colloid surface, some specific surface stabilizers (such as polyvinylpyrrolidone [27, 28]) or tedious three-step procedures (including surface activation with a silane coupling

[1] Author to whom any correspondence should be addressed.

agent, initial silica deposition with sodium silicate in aqueous solution, and extensive growth of silica shell with using the Stöber method) [26, 27] were needed. It is desirable to develop a facile procedure to synthesis colloidal silver–silica nanocomposites for MEF.

In this study, we developed a facile one-pot reverse microemulsion process to synthesize $Ag@SiO_2$ core–shell nanoparticles, in which two kinds of europium (Eu^{3+}) chelates were covalently doped in the silica shell; we then investigated the fluorescence enhancement of Eu^{3+} in such systems. The reverse microemulsion method has been used for coating inorganic nanoparticles (such as Ag [29], quantum dots [30] and iron oxide [31]) with silica. Compared with the Stöber method, it can better control the particle size and size distribution in a simple way. In comparison with the tedious methods usually reported in the literature to prepare the $Ag@SiO_2$ MEF system, our method is fast and easy to perform because formation of the silver nanoparticles, the *in situ* silica coating, and the doping of the silica shells with the Eu^{3+} chelates occur in the same microemulsion. We chose lanthanide chelates to take advantage of their intrinsic photophysical properties, such as long lifetimes, large Stokes shift, and sharp emission spectra that make them particularly advantageous for use as bio-labels compared with organic fluorophores [32]. The silica shell minimizes metal–fluorophore quenching effects, provides the matrix for covalent coupling of chelates, and in addition provides a wide variety of chemistries for biomolecule attachment. The facile synthesis procedure and the efficient enhanced fluorescence suggest this core–shell architecture has great potential for application in a variety of biological systems.

2. Methods

2.1. Materials

The non-ionic surfactant poly(oxyethylene) nonylphenyl ether (Igepal CO-520), silver nitrate ($AgNO_3$), tetraethoxysilane (TEOS, 99%), cyclohexane, ammonia (28–30 wt%), hydrazine hydrate ($N_2H_4{\cdot}xH_2O$), ethanol, iminodiacetic acid (IDA), dianhydride of diethylenetriaminepentaacetic acid (DTPA), *p*-aminobenzoic acid (PABA), 3-aminopropyltriethyloxysilane (APTS), 3-glycidoxypropyltrimethoxysilane (GLYMO) and europium nitrate hexahydrate ($Eu(NO_3)_3{\cdot}6H_2O$), 99.95% were all purchased from Sigma-Aldrich and used as received. De-ionized water was used for all experiments.

2.2. Synthesis of GLYMO–IDA silane precursor

The GLYMO–IDA silane was synthesized with a previously reported method [33] (figure 1(A)). IDA (4.25 g) was dissolved in 50 ml of de-ionized water, and the obtained solution was adjusted to pH 11.0 with 10 M NaOH. Then the solution was transferred into a flask bottle placed in the ice-bath at 0 °C, and 1.4 ml of GLYMO was slowly added under stirring. The mixed solution was heated to 65 °C for 6 h with stirring, and subsequently placed into an ice-bath for 5 min to decrease the temperature to 0 °C again, and 1.6 ml of GLYMO was added and mixed. Then the temperature of the solution was raised to 65 °C for another 6 h under stirring. Finally, the prepared GLYMO–IDA silane solution was adjusted to pH 6 with concentrated HCl.

2.3. Synthesis of PABA–DTPAA–APTS (PDA) silane precursor

PABA (0.19 g) was dissolved in 5 ml of DMSO. Then 0.5 g of DTPAA was added with vigorous stirring. After the mixture was stirred at room temperature for 8 h, 0.35 ml of APTS was added and the mixture was stirred overnight. The structure of PDA is shown in figure 1(B).

2.4. Synthesis of Eu^{3+}–GLYMO–IDA-doped $Ag@SiO_2$ core–shell nanoparticles and solid SiO_2 nanoparticles

Eu^{3+}–GLYMO–IDA-doped $Ag@SiO_2$ core–shell nanoparticles were prepared by a one-pot reverse microemulsion method [29] with some modifications (figure 1(C)). Typically, the water-in-oil (W/O) reverse microemulsion was formed at room temperature in a 50 ml three-neck flask consisting of 4 ml of Igepal CO-520, 10 ml cyclohexane, 0.94 ml 0.02 M silver nitrate solution under vigorous stirring. After 5 min, 50 μl of hydrazine hydrate reductant was added to the above mixture, followed by the addition of 25 μl ammonia. After another 10 min equilibration period, an appropriate stock solution of TEOS containing 50% TEOS and 50% cyclohexane by weight was injected into the microemulsion to initiate the polymerization reaction. After stirring for 24 h, 10 μl of TEOS and 20 μl of GLYMO–IDA silane were added, followed by adding 20 μl of ammonia. The reaction was continued for another 24 h under stirring. After the reaction was complete, the resulting core–shell nanostructures were isolated from the microemulsion by adding ethanol, followed by centrifuging and washing with ethanol and water successively for several times to remove the surfactants and other impurities. Eu^{3+}-doped nanoparticles were prepared by dispersing appropriate amount of the above nanoparticles in an aqueous solution of 5 ml of 0.01 M of $Eu(NO_3)_3$ with constant stirring overnight. Then the nanoparticles were centrifuged and washed with water several times. Solid SiO_2 nanoparticles without a Ag core served as a reference; they were also synthesized by the same method as above except without $AgNO_3$ in the aqueous phase during microemulsion formation.

2.5. Synthesis of Eu^{3+}–PDA-doped $Ag@SiO_2$ core–shell nanoparticles and hollow SiO_2 nanoparticles

PDA-doped $Ag@SiO_2$ core–shell nanoparticles were also synthesized in the W/O microemulsion system. In brief, the microemulsion was prepared by mixing 3.8 g of Igepal CO-520, 10 ml of cyclohexane and 0.5 ml of aqueous silver nitrate solution (0.01 M). After stirring for 30 min, 50 μl of hydrazine hydrate was added to the above mixture followed by the addition of 25 μl ammonia. 20 min later, 60 μl of TEOS was added into the microemulsion to initiate the polymerization reaction. The mixture was allowed to stir for 24 h, then 30 μl of TEOS and 20 μl of PADA silane precursor were added followed by adding 20 μl of ammonia. The reaction was continued for another 24 h under stirring.

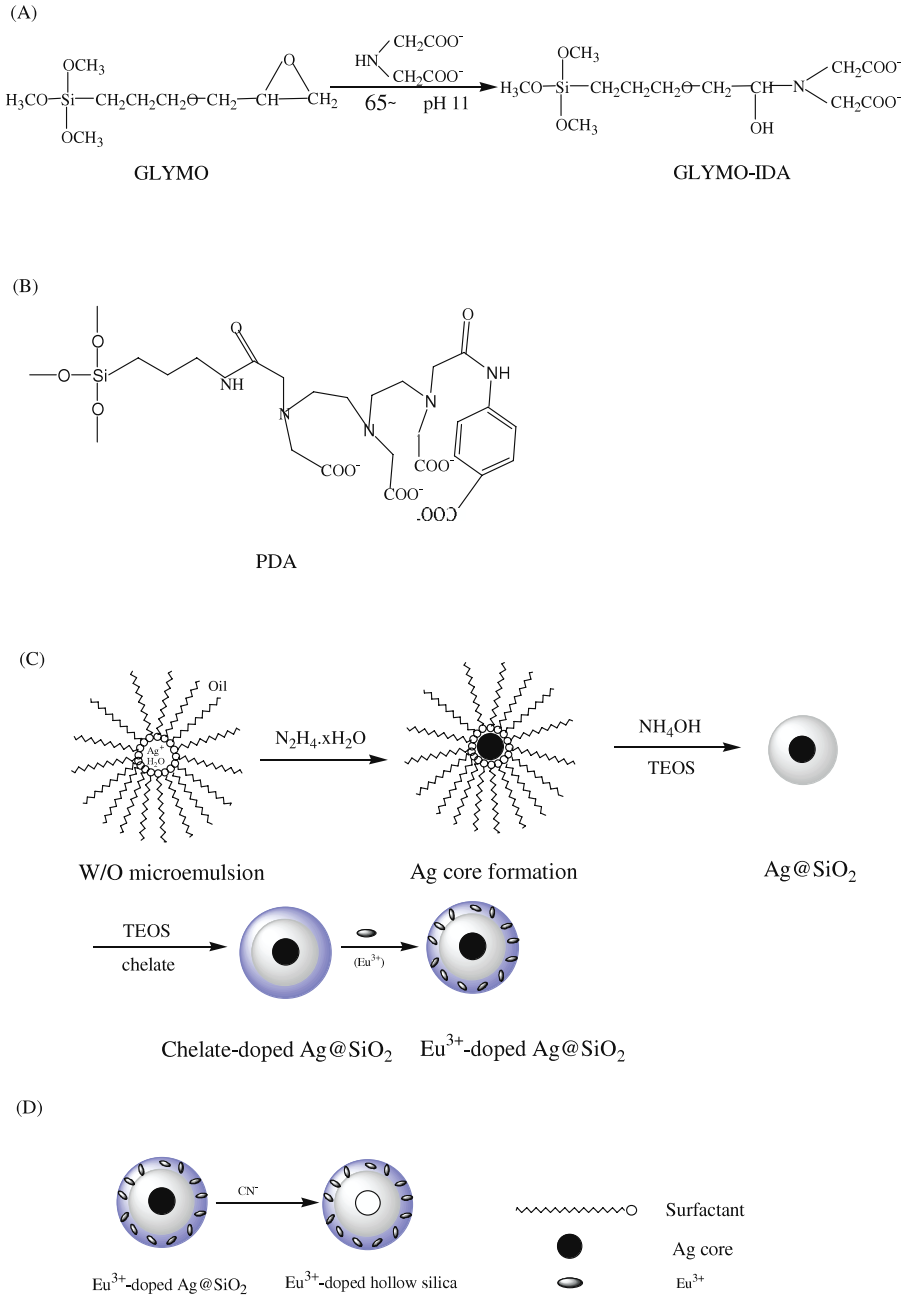

Figure 1. Schematic representation of (A) GLYMO–IDA silane; (B) PDA silane; (C) Synthesis of chelate-doped $Ag@SiO_2$ nanoparticles; (D) Synthesis of hollow SiO_2 nanoparticles.

The resulting nanoparticles were separated from the microemulsion by adding ethanol followed by centrifuging and washing with ethanol and water successively for several times. Then the nanoparticles were dispersed in 5 ml of 0.01 M of $Eu(NO_3)_3{\cdot}5H_2O$ solution and stirred overnight. The nanoparticles were then centrifuged, washed with H_2O and left to dry overnight. The silane precursor, PDA, an efficient chelating ligand for Eu^{3+}, was synthesized by conjugation of an organic chromophore, *p*-aminobenzoic acid (PABA) and a silane, 3-aminopropyl-triethyloxysilane (APTS) to a chelate, dianhydride of diethylenetriaminepentaacetic acid (DTPA). The structure of PDA is shown in figure 1(B). DTPA chelate serves as a scaffold for binding Eu^{3+} ions in close proximity to the organic chromophore (PABA), which captures the excitation light and sensitizes the lanthanide ion luminescent by fluorescence energy transfer; the APTS segment allows the precursor to be covalently linked to the silica matrix via copolymerization with TEOS, which prevents the leakage from the silica and ensures long-term stability of the fluorescence.

Hollow SiO_2 nanoparticles without a Ag core served as reference. Half of the above $Ag@SiO_2$ core shell nanoparticles were dispersed in 1 ml of 0.1 M sodium cyanide solution with stirring overnight to ensure complete etching of the silver cores from the particles. The resulting hollow silica nanoparticles were centrifuged and washed with water and ethanol under sonication several times to remove unreacted ions. The final

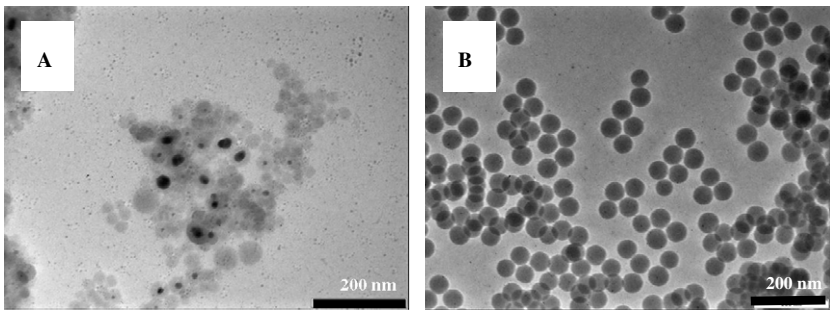

Figure 2. TEM images of (A) GLYMO–IDA-doped Ag@SiO_2 nanoparticles, (B) GLYMO–IDA-doped solid SiO_2 nanoparticles without Ag core.

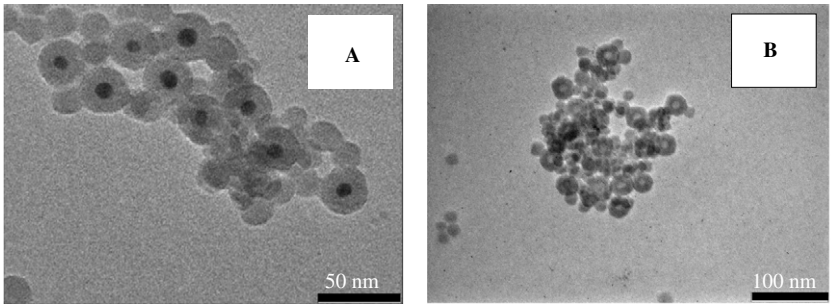

Figure 3. TEM images of (A) PDA-doped Ag@SiO_2 nanoparticles, (B) PDA-doped hollow silica nanoparticles without Ag core.

particles were suspended in water. Since the chelate complexes were covalently doped in the silica shell, the etching of silver core with cyanide ions did not cause leakage of the chelate complexes from the shell. This procedure permits the same amount of chelate to be excited in the presence and in the absence of the silver. Thus this allows for a more direct and precise evaluation of the impact of the nanosilver than could be achieved by using solid silica nanoparticles as a control.

2.6. Characterization

Absorption spectra and fluorescence spectra of samples in aqueous solution were measured with a Spectramax M2 cuvette/microplate reader (Molecular Devices). Emission lifetime was measured with a Roper Scientific thermoelectrically cooled, gated, intensified CCD camera mounted to a SpectraPro 150 spectrometer. The excitation source for the emission lifetime measurements was a diode pumped Nd:YAG laser that in turn pumped an optical parametric oscillator (OPO). The size and morphology of the samples was observed using transmission electron microscope (TEM, Philips CM-12). Samples were prepared by placing a drop of a dilute ethanol dispersion of the nanoparticles on the surface of a copper grid.

3. Results and discussion

The Ag@SiO_2 core–shell nanoparticles were successfully prepared using the facile one-pot microemulsion method beginning with silver nanoparticle formation, followed by *in situ* silica coating and fluorophore doping (figure 1(C)). It is notable that compared with other reports of lanthanide fluorescence enhancement, in which lanthanide chelates were mostly physically adsorbed in the silica matrix and thus may result in leakage, the chelates in our study were covalently immobilized in the silica shell by the silane agent, resulting in a very stable coupling that ensures long-term stability of the emission. To prepare GLYMO–IDA-doped Ag@SiO_2 nanoparticles, GLYMO–IDA silane precursor which has been demonstrated to be an efficient chelate for Eu^{3+} [34] was prepared by conjugation of an IDA chelate with a GLYMO silane that had epoxy groups. GLYMO was copolymerized with TEOS to make the precursor covalent immobilize in the silica matrix; the IDA group can chelate Eu^{3+} efficiently. The resulting core–shell nanoparticles reveal under TEM a dark Ag core and a light SiO_2 shell (figure 2(A)), confirming the formation of about 50 nm size core–shell nanocomposites with 20 nm Ag core and 15 nm silica shell. The images demonstrate the feasibility of using a microemulsion method for the synthesis of such core–shell structures.

To show the benefits of using a silver core in the fluorescent core–shell nanoparticles, we prepared control samples without the silver core. Figure 2(B) shows the TEM image of reference solid silica nanoparticles with a size of about 47 nm.

Figure 3 shows the TEM images of the as-prepared Ag@SiO_2 core–shell nanoparticles and hollow silica nanoparticles. Figure 3(A) clearly shows the nanoparticles having a core–shell structure with a dark contrast silver core (9 nm) and a light contrast silica shell (11 nm). The average size of the core–shell nanoparticles is about 30 nm. Figure 3(B) shows the TEM image of hollow silica nanoshells. It can be seen the Ag

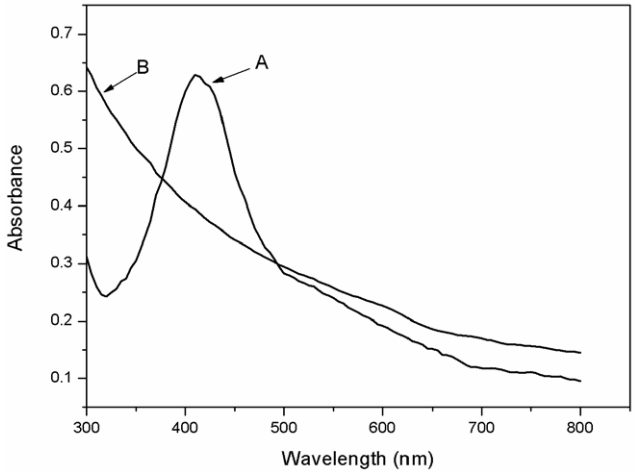

Figure 4. Absorption spectra of (A) GLYMO–IDA-doped Ag@SiO_2 nanoparticles and (B) GLYMO–IDA-doped solid SiO_2 nanoparticles without Ag core.

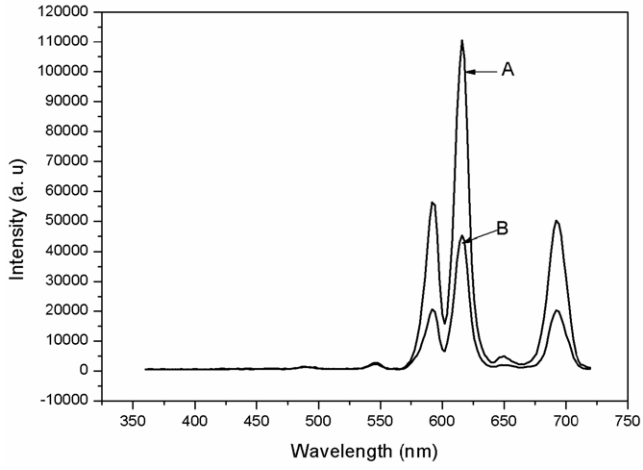

Figure 5. Fluorescence emission spectra of (A) Eu^{3+}–GLYMO–IDA-doped Ag@SiO_2 nanoparticles, (B) Eu^{3+}–GLYMO–IDA-doped solid silica nanoparticles without Ag core.

core has been etched away by cyanide ions, leaving a hollow core in the center.

Coating of the silver core with a silica shell is advantageous for applications in biological system, because silica surfaces are highly biocompatible and are easy to functionalize and conjugate with biomolecules and fluorophores based on well-established silica surface chemistry. Most importantly, silica here provides a suitable fluorophore–metal distance or spacer which is important for the distance dependent MEF phenomenon. Many researchers have proved that the metal nanoparticles can exhibit fluorescence enhancement only with sufficiently large distances between the fluorophore and the metal surface [35], while fluorescence is quenched by direct contact of the fluorophore with a Ag surface [27]. For this reason, we doped the Eu^{3+} chelates in the silica shell which acts as a spacer to avoid quenching for most of the europium ions.

Figure 4 shows the absorption spectra of GLYMO–IDA–Eu^{3+}-doped Ag@SiO_2 core–shell nanoparticles and solid SiO_2 nanoparticles (reference). The surface plasmon resonance (SPR) peak of the silver can be seen at 415 nm, which is similar to the value reported in [36], whereas the solid silica nanoparticles show no plasmon absorption band, further confirming that the silver cores have been successfully formed in the core–shell nanostructures. The emission spectra of solutions of Eu^{3+}-doped Ag@SiO_2 nanoparticles and of Eu^{3+}-doped SiO_2 nanoparticles are presented in figure 5. All spectra were recorded with 260 nm excitation. Both samples showed identical characteristic emission peaks of Eu^{3+} at 592, 615, 653 and 694 nm, respectively, of which 615 nm was the most prominent one, indicating that Eu^{3+} was strongly chelated in the silica shell and the spectral properties of Eu^{3+} were retained in the presence of the silver core. The four peaks were due to the transitions from the $^5D_0$ level to ^7F_J ($J = 1, 2, 3, 4$) levels, respectively. The Ag@SiO_2 nanoparticles showed about a 3-fold fluorescence enhancement compared to the silver free nanoparticles. The distinct emission band at 615 nm for Eu^{3+} can be observed in both samples.

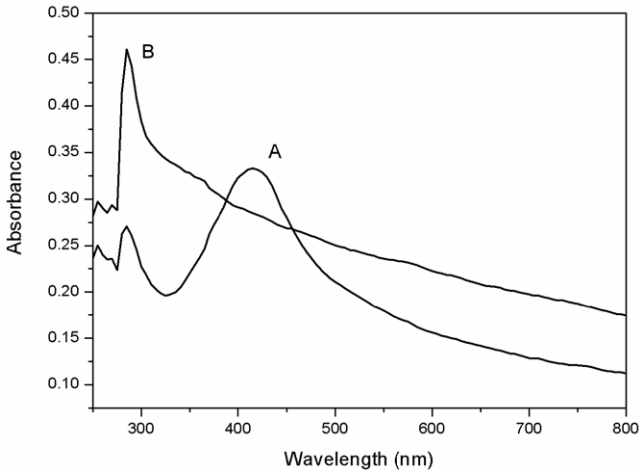

Figure 6. Absorption spectra of (A) Eu^{3+}–PDA-doped Ag@SiO_2 nanoparticles, (B) Eu^{3+}–PDA-doped hollow SiO_2 nanoparticles without Ag core.

This finding clearly shows that the silver nanoparticles can produce fluorescence enhancement when the silica serves as a separation layer between the Eu^{3+} chelate and the silver core. Fluorescence lifetime measurements showed a reduction in lifetime for Ag@SiO_2 nanoparticles as compared to Ag free nanoparticles. The mean lifetime is reduced from 1.15 ms in Ag free nanoparticles to 0.9 ms in Ag@SiO_2 nanoparticles, an approximate 1.3-fold reduction. These observations are in accordance with other reports about the silver nanoparticles for the MEF of lanthanide chelates [26, 37].

Figure 6 shows the absorption spectra of Eu^{3+}–PDA-doped Ag@SiO_2 core–shell nanoparticles and control hollow silica nanoparticles. Strong absorption at 285 nm is observed for both samples, which is due to the absorption of europium complex, indicating that the covalent incorporation of europium complex in core–shell nanoparticles is feasible using a silane precursor. The SPR peak of the silver can also be seen from the Ag@SiO_2 nanoparticles at 415 nm.

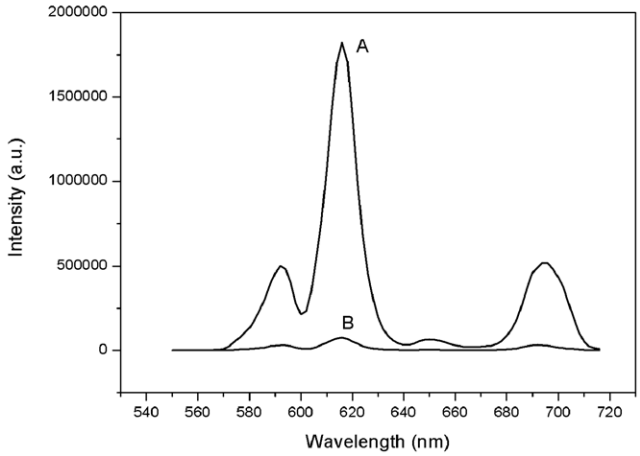

Figure 7. Fluorescence emission spectra of (A) Eu^{3+}–PDA-doped $Ag@SiO_2$ nanoparticles, (B) Eu^{3+}–PDA-doped hollow SiO_2 nanoparticles without Ag core.

The hollow silica nanoparticles, however, do not display a plasmon absorption band, whereas the absorption band caused by the europium complex is still present, confirming that the silver has been successfully etched away by cyanide with no impact on the doped fluorophore. Figure 7 shows the emission spectra (excitation at 260 nm) from Eu^{3+}–PDA-doped $Ag@SiO_2$ nanoparticles and Eu^{3+}-doped hollow silica nanoparticles (control sample) without Ag core. Both samples showed identical characteristic emission peaks of Eu^{3+} at 592, 615, 653 and 694 nm, respectively, of which 615 nm was the most prominent one. This indicated that the treatment with cyanide ions had no impact on the spectral properties of the fluorophores. The emission intensity was approximately 24-fold higher for $Ag@SiO_2$ nanoparticles than hollow silica nanoparticles. The presence of a Ag core in the core–shell nanoparticles also resulted in a reduction of the emission lifetime compared to the hollow silica particles. The average lifetimes of $Ag@SiO_2$ nanoparticles and hollow silica nanoparticles were measured to be 1.05 and 1.26 ms, respectively.

The outcome of MEF results in an increase in the quantum yield (i.e., emission intensity) and a decrease in the lifetime of fluorophores. This corresponds to our observations, which show that the fluorescence intensity is higher, and the fluorescence lifetime is shorter, for Eu^{3+}-doped $Ag@SiO_2$ nanoparticles than for coreless silica nanoparticles. The metal–fluorophore interactions are due to an enhanced local electric field with an increase in the intrinsic system decay rate. The first factor provides stronger excitation rates but does not modify the fluorescence lifetime of the fluorophores. The second factor increases the system radiative decay rate (thus the lifetime is reduced), leading to the increase of the net fluorophore quantum yield [26, 37]. The reduction in lifetime as well as an increase in fluorescence emission intensity is particularly interesting for fluorescence-based applications where a 24-fold increase in intensity coupled with a 1.2-fold reduction in lifetime, provides for an about 28-fold potential increase in overall particle detectability [26]. Moreover, a reduced lifetime affords increased fluorophore photostability, as there is less time for excited state photodestructive processes to occur such as oxidation, interaction with singlet oxygen or even superoxide [26]. Our results show that it is important to employ an appropriate chelate in order to achieve the greatest enhancement of the emission. The exact nature of the role of the chelate chemistry in determining the extent of enhancement remains to be resolved.

4. Conclusions

Eu^{3+}-doped $Ag@SiO_2$ core–shell nanoparticles have been synthesized using a facile one-pot microemulsion method for potential applications with metal enhanced fluorescence. The presence of a Ag core can result in as much as a 24-fold increase in emission intensity compared with silica nanoparticles without silver, which may permit greater detectability and thus better sensitivity for solution-based sensing. It is feasible that our nanoparticle synthesis strategy will allow doping of a wide variety of fluorophores into the silica shell by a one-pot microemulsion system—while exploiting the benefits of using a metal core for MEF. The form of the chelate has a major impact on the extent of enhancement that can be achieved by the use of a silver core.

Acknowledgments

This publication was made possible by grant number 5 P42 ES004699 from the National Institute of Environmental Health Sciences (NIEHS), NIH and the contents are solely the responsibility of the authors and do not necessarily represent the official views of the NIEHS, NIH. The project was also supported by the National Research Initiative of the USDA Cooperative State Research, Education and Extension Service, grant number 2009-35603-05070.

References

[1] Dubertret B, Calame M and Libchaber A J 2001 Single-mismatch detection using gold-quenched fluorescent oligonucleotides *Nat. Biotechnol.* **19** 365–70
[2] Ray K, Badugu R and Lakowicz J R 2006 Metal-enhanced fluorescence from CdTe nanocrystals: a single-molecule fluorescence study *J. Am. Chem. Soc.* **128** 8998–9
[3] Louis C, Roux S, Ledoux G, Lemelle L, Gillet P, Tillement O and Perriat P 2004 Gold nano-antennas for increasing luminescence *Adv. Mater.* **16** 2163–6
[4] Sokolov K, Chumanov G and Cotton T M 1998 Enhancement of molecular fluorescence near the surface of colloidal metal films *Anal. Chem.* **70** 3898–905
[5] Malicka J, Gryczynski I, Geddes C D and Lakowicz J R 2003 Metal-enhanced emission from indocyanine green: a new approach to *in vivo* imaging *J. Biomed. Opt.* **8** 472–8
[6] Aslan K, Huang J, Wilson G M and Geddes C D 2006 Metal-enhanced fluorescence-based RNA sensing *J. Am. Chem. Soc.* **128** 4206–7
[7] Malicka J, Gryczynski I and Lakowicz J R 2003 DNA hybridization assays using metal-enhanced fluorescence *Biochem. Biophys. Res. Commun.* **306** 213–8
[8] Matveeva E, Gryczynski Z, Malicka J, Gryczynski I and Lakowicz J R 2004 Metal-enhanced fluorescence

immunoassays using total internal reflection and silver island-coated surfaces *Anal. Biochem.* **334** 303–11
[9] Matveeva E G, Gryczynski Z and Lakowicz J R 2005 Myoglobin immunoassay based on metal particle-enhanced fluorescence *J. Immunol. Methods* **302** 26–35
[10] Lakowicz J R 2001 Radiative decay engineering: biophysical and biomedical applications *Anal. Biochem.* **298** 1–24
[11] Lakowicz J R 2005 Radiative decay engineering 5: metal-enhanced fluorescence and plasmon emission *Anal. Biochem.* **337** 171–94
[12] Lakowicz J R 2006 Plasmonics in biology and plasmon-controlled fluorescence *Plasmonics* **1** 5–33
[13] Lakowicz J R *et al* 2004 Advances in surface-enhanced fluorescence *J. Fluoresc.* **14** 425–41
[14] Fort E and Gresillon S 2008 Surface enhanced fluorescence *J. Phys. D: Appl. Phys.* **41** 1–31
[15] Xie F, Baker M S and Goldys E M 2006 Homogeneous silver-coated nanoparticle substrates for enhanced fluorescence detection *J. Phys. Chem.* B **110** 23085–91
[16] Aslan K and Geddes C D 2005 Microwave-accelerated metal-enhanced fluorescence: platform technology for ultrafast and ultrabright assays *Anal. Chem.* **77** 8057–67
[17] Aslan K, Badugu R, Lakowicz J R and Geddes C D 2005 Metal-enhanced fluorescence from plastic substrates *J. Fluoresc.* **15** 99–104
[18] Gryczynski I, Malicka J, Gryczynski Z, Lakowicz J R and Geddes C D 2002 Dramatic increases in resonance energy transfer have been observed between fluorophores bound to DNA above metallic silver islands: opportunities for long-range immunoassays and new DNA arrays *J. Fluoresc.* **12** 131–3
[19] Geddes C D, Cao H, Gryczynski I, Gryczynski Z, Fang J Y and Lakowicz J R 2003 Metal-enhanced fluorescence (MEF) due to silver colloids on a planar surface: potential applications of indocyanine green to *in vivo* imaging *J. Phys. Chem.* A **107** 3443–9
[20] Aslan K, Leonenko Z, Lakowicz J R and Geddes C D 2005 Fast and slow deposition of silver nanorods on planar surfaces: application to metal-enhanced fluorescence *J. Phys. Chem.* B **109** 3157–62
[21] Parfenov A, Gryczynski I, Malicka J, Geddes C D and Lakowicz J R 2003 Enhanced fluorescence from fluorophores on fractal silver surfaces *J. Phys. Chem.* B **107** 8829–33
[22] Ray K, Badugu R and Lakowicz J R 2006 Distance-dependent metal-enhanced fluorescence from Langmuir–Blodgett monolayers of alkyl-NBD derivatives on silver island films *Langmuir* **22** 8374–8
[23] Geddes C D, Parfenov A, Roll D, Fang J Y and Lakowicz J R 2003 Electrochemical and laser deposition of silver for use in metal-enhanced fluorescence *Langmuir* **19** 6236–41
[24] Pompa P P, Martiradonna L, la Torre A, la Sala F, Manna L, De Vittorio M, Calabi F, Cingolani R and Rinaldi R 2006 Metal-enhanced fluorescence of colloidal nanocrystals with nanoscale control *Nat. Nanotechnol.* **1** 126–30
[25] Aslan K, Lakowicz J R, Szmacinski H and Geddes C D 2004 Metal-enhanced fluorescence solution-based sensing platform *J. Fluoresc.* **14** 677–9
[26] Aslan K, Wu M, Lakowicz J R and Geddes C D 2007 Fluorescent core–shell Ag@SiO_2 nanocomposites for metal-enhanced fluorescence and single nanoparticle sensing platforms *J. Am. Chem. Soc.* **129** 1524–5
[27] Tovmachenko O G, Graf C, van den Heuvel D J, van Blaaderen A and Gerritsen H C 2006 Fluorescence enhancement by metal-core/silica-shell nanoparticles *Adv. Mater.* **18** 91–5
[28] Graf C, Vossen D L J, Imhof A and van Blaaderen A 2003 A general method to coat colloidal particles with silica *Langmuir* **19** 6693–700
[29] Li T, Moon J, Morrone A A, Mecholsky J J, Talham D R and Adair J H 1999 Preparation of Ag/SiO_2 nanosize composites by a reverse micelle and sol–gel technique *Langmuir* **15** 4328–34
[30] Darbandi M, Thomann R and Nann T 2005 Single quantum dots in silica spheres by microemulsion synthesis *Chem. Mater.* **17** 5720–5
[31] Yi D K, Selvan S T, Lee S S, Papaefthymiou G C, Kundaliya D and Ying J Y 2005 Silica-coated nanocomposites of magnetic nanoparticles and quantum dots *J. Am. Chem. Soc.* **127** 4990–1
[32] Ye Z Q, Tan M Q, Wang G L and Yuan J L 2004 Novel fluorescent europium chelate-doped silica nanoparticles: preparation, characterization and time-resolved fluorometric application *J. Mater. Chem.* **14** 851–6
[33] Ma Z Y, Guan Y P and Liu H Z 2006 Superparamagnetic silica nanoparticles with immobilized metal affinity ligands for protein adsorption *J. Magn. Magn. Mater.* **301** 469–77
[34] Lis S and Choppin G R 1995 Luminescence study of europium(Iii) complexes with several dicarboxylic-acids in aqueous-solution *J. Alloys Compounds* **225** 257–60
[35] Schneider G, Decher G, Nerambourg N, Praho R, Werts M H V and Blanchard-Desce M 2006 Distance-dependent fluorescence quenching on gold nanoparticles ensheathed with layer-by-layer assembled polyelectrolytes *Nano Lett.* **6** 530–6
[36] Kobayashi Y, Katakami H, Mine E, Nagao D, Konno M and Liz-Marzan L M 2005 Silica coating of silver nanoparticles using a modified Stober method *J. Colloid Interface Sci.* **283** 392–6
[37] Wu M, Lakowicz J R and Geddes C D 2005 Enhanced lanthanide luminescence using silver nanostructures: opportunities for a new class of probes with exceptional spectral characteristics *J. Fluoresc.* **15** 53–9